DSC-Vol. 64, Proceedings of the ASME
Dynamic Systems and Control Division
ASME 1998

MINIMUM MASS FOR HAPTIC DISPLAY SIMULATIONS

J. Michael Brown
J. Edward Colgate

Department of Mechanical Engineering
Northwestern University
Evanston, IL 60208, USA

mb@nwu.edu colgate@nwu.edu

ABSTRACT

This paper addresses the issue of providing stability guarantees during the implementation of multibody simulations for haptic display. Within the framework of the virtual coupling, we discuss the passivity of the haptic display. Previous work has established that, if the numerical methods used in the virtual environment are discrete time passive, it is possible to decouple the stability of the device from the virtual environment simulation. In the present work, we prove that discrete time passive operators must be implicit, making them unlikely candidates for real time implementation. Given restrictions on environment parameters, however, passivity can sometimes be preserved even when using explicit numerical methods. An important benchmark simulation is that of a point mass, and restrictions take the form of a minimum mass that can be simulated passively. This minimum mass is derived for several simple numerical integrator-virtual coupling pairs.

1. INTRODUCTION

Many of the proposed applications for haptic displays involve the simulation of a complex dynamic system (e.g. aeronautical training and virtual prototyping). This simulation must then be interfaced with a haptic display so that information about forces and motions can be exchanged haptically between the human user and the virtual environment. To date, however, virtual environments from published works have consisted primarily of haptic primitives, like virtual walls (Colgate, et al., 1993, Salcudean and Vlaar, 1994), masses, and simple textures (Howe and Cutkosky, 1993, Klatzky, et al., 1989, Minsky, 1995). Other implementations include (Zilles and Salisbury, 1995), which describes an approach to the implementation of complex static environments, but does not address the extension to dynamic environments. Gillespie (1996) describes the implementation of complex dynamic environments whose constraint configurations are known a priori. In recent years, our group has been working on the development of a general purpose multibody simulator for haptic display (Brown and Colgate, 1997, Chang and Colgate, 1997, Colgate, et al., 1995).

A major impediment to the development of complex simulations is the difficulty of providing *stability guarantees* when working with haptic virtual environments. These guarantees are important both because instabilities are potentially dangerous and because they typically destroy the user's sense of immersion. Most existing virtual environments rely on the careful tuning of environment and control parameters to ensure stability. Whenever changes are made to the environment (such as changing the length of an object), these parameters have to be re-tuned. While merely annoying for relatively simple environments, this process becomes impractical for complex ones.

In the effort to build complex multibody environments for haptic interface, a natural starting point is the physics-based simulation literature. This literature pulls from several different research communities: computer graphics, robotics, and applied mechanics. In recent years, it has produced a variety of modeling and implementation tools for use with multibody computer simulations. However, since these tools were not designed with haptic interface in mind, it is not clear that they will work properly when used in this context. For a review of multibody simulation formalisms and their applicability to haptic interface, see (Gillespie, 1997).

Our own experience has indicated that algorithms which work well with stand-alone simulations often fail when implemented with a haptic display. One cause of this failure is the difficulty of obtaining stability guarantees for any usefully broad class of environments. To address this difficulty, it would be useful to develop a general-purpose software and hardware architecture for real-time haptic interaction between

users and complex dynamic simulations. Ideally, this architecture would decouple the haptic display from the multibody simulation, such that stability of the haptic display is not strongly dependent on simulation parameters. Our goal is to allow a knowledgeable user (but not an expert in haptic display) to design virtual environments while maintaining confidence that the resultant system will be stable.

One difficulty in any traditional stability analysis of this system is the dynamics of the human operator. Even though the virtual environment itself might be stable, interaction with a human operator via a haptic interface may cause instability. In our studies of virtual environments, we have had many experiences with human operators adjusting their own behavior until oscillations resulted. Another approach to proving robustness is to derive the conditions under which the haptic display handle appears *passive* to the human operator. Under these conditions, the device cannot generate energy continually over time, making actuator-driven instabilities impossible. This approach is elegant because it doesn't rely on a model of the human operator dynamics.

Previous work in this area has established that, by using a virtual coupling, the passivity of the haptic display can be largely decoupled from the virtual environment parameters(Brown and Colgate, 1997). One of the assumptions made in the analysis was that the virtual environment be discrete-time passive. It was shown that numerical integrators and collision response algorithms which conserve energy will meet this property.

In this paper, we prove that discrete time passive numerical methods must be implicit, requiring an iterative solution process when used with the virtual coupling. We demonstrate that, by restricting the mass of the virtual tool to be greater than a given value, passivity can be maintained even with explicit numerical methods. In Section 2, we review the structure of a haptic display simulation based on the virtual coupling between the manipulandum and the multibody simulation, highlighting important previous results. Section 3 explores in detail the passivity of a simulation of a point mass, and demonstrates that any given haptic display has a minimum mass that it can simulate using explicit integration methods. Finally, Section 4 reviews a haptic display tuning process and briefly outlines experiments currently under way to verify the approach.

2. REVIEW OF THE VIRTUAL COUPLING

Every haptic display has a finite range of impedances that it can render passively. This range of impedances, called the Z-width, is affected by a number of factors, including inherent mechanism dynamics, controller update rate, and sensor/actuator performance. To ensure system robustness, the haptic display hardware must never be commanded to render an impedance that is outside its Z-width. One way of achieving this goal is to design virtual environments so that all contacts are compliant. Problems arise with this method because these compliances are modulated by the geometry of the simulated environment. This modulation results in stability properties that are geometry dependent and sub-optimal. Additionally, simulations must be designed for a particular device, resulting in poor portability.

First proposed in (Colgate, et al., 1995) as a more general approach to the implementation of complex virtual environments, the virtual coupling addresses the problems mentioned above. Shown in Figure 1 as a multi-dimensional spring and damper, the virtual coupling allows the environment design to be separated from the sampled-data control issues associated with haptic display. Instead of putting the compliance between the virtual tool and its environment, the compliance is between the haptic display hardware and the virtual tool. The virtual coupling acts like an

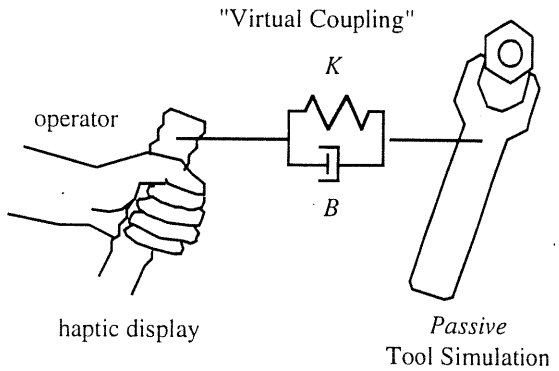

Figure 1. Conceptualization of a virtual coupling in a hand tool simulation. The spring and damper form a connection between the haptic display handle and the multibody simulation, transmitting force and motion between them.

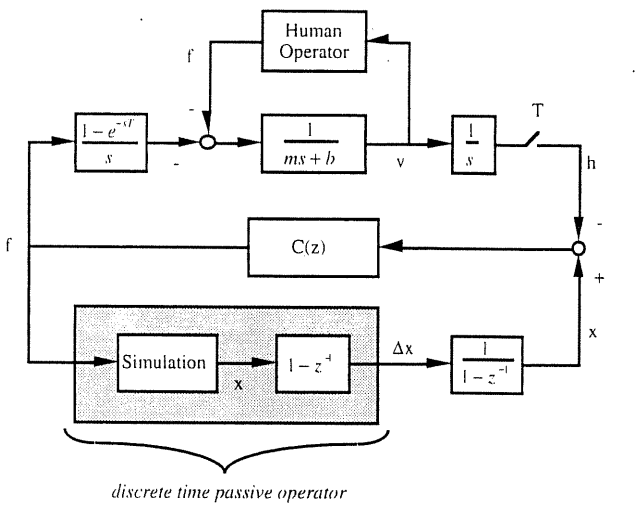

Figure 2. Model of a haptic display, including sample/hold, mechanism, human operator, and virtual environment dynamics. *C(z)* is the virtual coupling, *m* and *b* are the mass and damping of the haptic display mechanism, *T* is the sample time, *h* is the position of the handle, *x* is the position of the environment side of the virtual coupling, and *f* is the virtual coupling force.

impedance filter, limiting the rendered impedances to within the Z-width of the particular device being used. If the virtual environment calls for an infinite stiffness to be displayed, such as when a rigid wrench interacts with a rigid bolt, the device will render the impedance of the virtual coupling.

The conceptual separation of the virtual environment from the rest of the haptic display system permits a rigorous passivity analysis for a large class of simulations, allowing stability conditions to remain relatively independent of simulation parameters. In (Brown and Colgate, 1997), the results were extended to arbitrary linear virtual couplings and environments with non-linear dynamics . Figure 2 shows the model used in the analysis of a 1 DOF haptic display. While it incorporates a very simple model of inherent device dynamics, its strength is a rigorous model of the sample-hold dynamics.

The primary analytic result was a derivation of the conditions under which the haptic display handle appears passive to the human operator. If the virtual environment dynamics are discrete-time passive, then the passivity condition for the haptic display is:

$$b > \frac{T}{2} \frac{1-\cos\omega T}{\mathrm{Re}\left\{\frac{1-e^{-j\omega T}}{C\left(e^{j\omega T}\right)}\right\}} \qquad (1)$$

This result shows that discrete-time passive numerical methods allow the development of passivity conditions which are independent of environment parameters for any linear virtual coupling. Further, it provides an analytical tool for evaluating the performance of a given coupling.

A similar approach is taken in (Adams, et al., 1998), which uses a 2-port virtual coupling network to achieve the same type of separation between the haptic display hardware and virtual environment simulation. Because the model of sample-hold is simpler than the one used in the present work, broader results can be obtained. It is unclear, however, whether the simplified model of sample-hold significantly compromises the accuracy of the results.

3. MINIMUM MASS OF HAPTIC DISPLAY SIMULATIONS

A critical assumption made in previous passivity analyses of virtual couplings is that the virtual environment be discrete-time passive. After exploring the effect of discrete-time passivity on numerical integrators and collision response algorithms, (Brown and Colgate, 1997) observed that an explicit discrete-time passive integrator had not been found. Section 3.1 reviews the importance of explicit and implicit numerical operators when used in a real-time context. Section 3.2 proves that explicit discrete-time passive numerical operators do not exist. Section 3.3 explores specific discrete-time active numerical methods when used with the virtual coupling, and establishes the minimum mass that can be simulated with specific integrator-virtual coupling pairs.

3.1 Explicit vs. implicit integrators

A numerical operator is implicit if its inputs at the *kth* step depend on the outputs at the *kth* step. Since the virtual environment output immediately affects the input (via the virtual coupling), the integrator will be implicit unless it has at least a one time step delay. This characteristic has important ramifications both for discrete-time passivity and for software implementation.

Figure 3 shows the discrete portion of a haptic display simulating a 1 DOF point mass and using an explicit Euler integrator with a spring-damper virtual coupling. By looking at the transfer function from f to x, we can see that x_k does not depend on f_k, but rather on f_{k-2}. This dependence means that the calculation at each sample time can be broken into two steps. The first is to calculate f_k (which does not depend on x_k). This force is then sent back to the haptic display hardware and also to the environment simulation. The second step is to calculate x_k. This new mass position will not be used until two more position measurements arrive from the sensors.

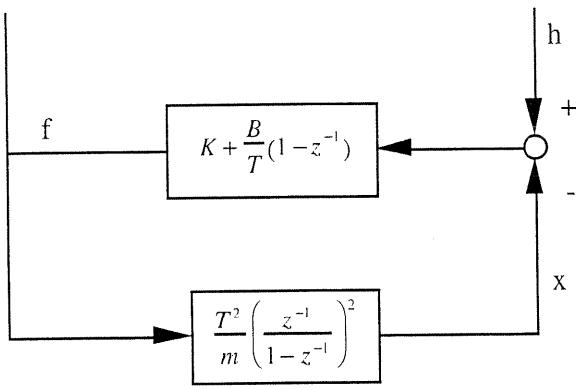

Figure 3. Backwards difference spring-damper virtual coupling and virtual mass with explicit Euler integration.

Figure 4 again shows the discrete portion of a haptic display simulating a 1 DOF point mass. This time, however, it is using an implicit Euler integrator with the spring-damper virtual coupling. The primary difference is that x_k now depends directly on f_k, making it impossible to split the calculation into two distinct steps. There are two approaches to calculating f_k: combination and iteration. In combination, we calculate f as a function of h directly through block diagram manipulation, which can then be converted into difference equations. The extension to more complicated environments, where integration, collision detection, and collision response are all combined into one formulation, makes this approach unworkable. Iteration is the normal technique used to solve implicit equations, but would require extremely careful consideration of efficiency and convergence due to the unilateral constraints present in multibody simulations.

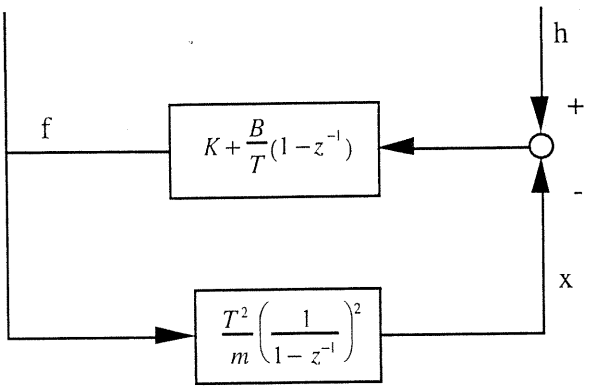

Figure 4. Backwards difference spring-damper virtual coupling and virtual mass with implicit Euler integration.

3.2 Discrete time passive numerical operators

We now turn our attention to whether there exists explicit discrete time passive numerical integrators. Such an integrator would be ideal, as it would lead to good stability properties and could be implemented easily in real time. Consider an arbitrary discrete operator G acting on input u and resulting in output y:

$$y_k = G(u_k, y_{k-1}, u_{k-1}, y_{k-2}, u_{k-2}, \ldots, y_1, u_1, y_0, u_0) \quad (2)$$

Both u and y are assumed to be zero for negative values of k. If G is explicit, then the dependence of y_k on u_k is removed:

$$y_k = G(y_{k-1}, u_{k-1}, y_{k-2}, u_{k-2}, \ldots, y_1, u_1, y_0, u_0) \quad (3)$$

From basic passivity definitions given in (Desoer and Vidyasagar, 1975), G is discrete-time passive iff:

$$\sum_{k=0}^{N} u_k \cdot y_k \geq -E_0 \qquad \forall N \in \mathbb{Z}^+ \quad (4)$$

which can be rewritten as:

$$u_N y_N \geq -E_0 - \sum_{k=0}^{N-1} u_k \cdot y_k \qquad N \in \mathbb{Z}^+ \quad (5)$$

Since y_N depends only on previous values of u and y, we can select u_N such that this expression will be violated:

$$y_N > 0 : \; u_N < -\frac{E_0 + \sum_{k=0}^{N-1} u_k y_k}{y_N} \quad (6)$$

$$y_N < 0 : \; u_N > -\frac{E_0 + \sum_{k=0}^{N-1} u_k y_k}{y_N} \quad (7)$$

The only case where u_N cannot be selected to violate (4) is trivial, when $y_N=0$ for all N. Since any non-trivial explicit method cannot be discrete-time passive, it follows that all discrete-time passive numerical operators must be implicit. It should be noted that the converse is false; not all implicit methods are discrete-time passive.

3.3 Explicit Numerical Methods

Since discrete time passive methods are difficult to implement in practice and anecdotal evidence indicates that explicit (and thus discrete time active) methods are often satisfactory, we need to formulate a new approach to proving robustness. As an exploration into this topic, consider the simulation of a 1-DOF point mass, with the usual virtual coupling structure outlined in Section 2. In addition to being a good way of exploring the passivity theory for more general systems, the simulation of a mass is one of the critical building blocks for multibody simulations. This analysis will use a backwards-difference spring-damper virtual coupling and three different numerical integrators. These numerical methods will be compared with a backwards-difference spring-damper virtual wall. Since all the virtual coupling and environment operators are linear, the derivations are straight forward using standard linear passivity tools.

3.3.1 Passivity of the virtual wall

(Colgate and Schenkel, 1997) analyzed the system shown in Figure 5.

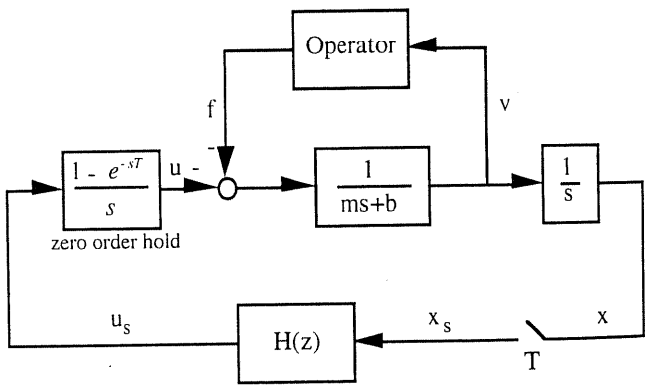

Figure 5. Model used to analyze a 1 DOF haptic display with linear environment dynamics, where *m* and *b* are the mass and damping of the haptic display hardware, *x* and *v* are the position and velocity of the handle, *u* is the motor torque, *f* is the handle force, *T* is the sample time, and *H(z)* is the virtual environment.

The most general result was an expression for the minimum physical damping necessary to ensure that the device would appear passive to the human operator, assuming linear virtual environment dynamics:

$$b > \frac{T}{2}\frac{1}{1-\cos\omega T}\,\mathrm{Re}\left\{\left(1-z^{-1}\right)H(z)\right\}_{z=e^{j\omega T}} \qquad (8)$$
$$0 \le \omega \le \omega_s$$

This result was used to obtain the passivity condition for a backwards-difference implementation of a spring-damper wall with stiffness K and damping B:

$$H(z) = K + \frac{B}{T}\left(1-z^{-1}\right) \qquad (9)$$

resulting in the following passivity condition:

$$b > \frac{KT}{2} + B \qquad (10)$$

To simplify comparisons with simulations of masses, it is useful to use a dimensionless parameter, β, to indicate the relative amount of virtual damping compared to virtual stiffness:

$$\beta = \frac{B}{KT} \qquad (11)$$

Using this substitution, the transfer function and passivity condition become:

$$H(z) = K\left(1+\beta-\beta z^{-1}\right) \qquad (12)$$

$$b > \frac{KT}{2}(1+2\beta) \qquad (13)$$

We will use this result as a benchmark for comparison. In the following subsections, we derive the conditions under which the simulation of a point mass has the same passivity condition as the virtual wall.

3.3.2 Simulation of a point mass

Comparison between Figures 2 and 5, yields the combined expression for virtual coupling, $C(z)$, and environment, $E(z)$, dynamics:

$$H(z) = \frac{C(z)}{1+C(z)E(z)} \qquad (14)$$

We will consider three different numerical integrators (see Table 1). All three methods use explicit Euler integration to update velocity, making them all discrete-time active. Before proceeding, we will introduce a second dimensionless parameter, α, representing the natural frequency associated

Numerical Method	Difference Equations	Discrete Transfer Function
Exp Euler velocity Exp Euler position	$v_k = v_{k-1} + \frac{T}{m_e} f_{k-1}$ $x_k = x_{k-1} + T v_{k-1}$	$\frac{x(z)}{f(z)} = \frac{T^2}{m_e}\frac{z^{-2}}{\left(1-z^{-1}\right)^2}$
Exp Euler velocity Imp Euler position	$v_k = v_{k-1} + \frac{T}{m_e} f_{k-1}$ $x_k = x_{k-1} + T v_k$	$\frac{x(z)}{f(z)} = \frac{T^2}{m_e}\frac{1}{\left(1-z^{-1}\right)^2}$
Exp Euler velocity Trap position	$v_k = v_{k-1} + \frac{T}{m_e} f_{k-1}$ $x_k = x_{k-1} + T\frac{v_{k-1}+v_k}{2}$	$\frac{x(z)}{f(z)} = \frac{T^2}{2m_e}\frac{\left(1+z^{-1}\right)z^{-1}}{\left(1-z^{-1}\right)^2}$

Table 1. Transfer functions and difference equations of explicit numerical integrators

with the virtual coupling's spring and the virtual environment's mass, scaled against the update rate of the controller:

$$\alpha = \frac{KT^2}{m_e} \qquad (15)$$

Substituting the transfer functions from Table 1 into (8) results in a passivity condition for each of the implementations. These passivity conditions can be compared to (13), yielding the minimum physical damping necessary to ensure passivity (see Appendix for details). While difficult to calculate analytically, Figures 6-8 show the regions in α-β space where the passivity condition for each simulation matches that of the virtual wall. The figures use level curves of the ratio of the required damping for each mass simulation to the required damping for the virtual wall. In regions where the ratio is less than or equal to unity, (13) is sufficient to determine passivity. In essence, the ratio is an indication of activeness, relative to the activeness of the virtual wall.

To interpret these graphs, it is useful to step through the environment design process in terms of the dimensioned parameters, K, B, m, and T. Selection of the stiffness, damping and update rate determines β, and thus the position on the abscissa, along with the scale factor of $1/m$ on the ordinate. Regardless of this selection, decreasing m will eventually lead to crossing the unity level curve (i.e., exceeding the damping necessary for the virtual wall). Increasing m will result in α approaching zero, where the required damping matches that of the virtual wall. Notable features of these graphs include:

- For Method 1 (Figure 6), β must be greater than one to achieve passivity
- For Method 2 (Figure 7), more damping is always required for mass simulations than for virtual walls. However, the gradient of the required damping is fairly low, so that if the virtual wall is allowed to be somewhat softer than optimal, a reasonable range of masses can be simulated passively.

- For Method 3 (Figure 8), β must be greater than *1/2* to achieve passivity. The region under the unity level curve is flat, indicating that the values of α and β do not affect passivity within this region.

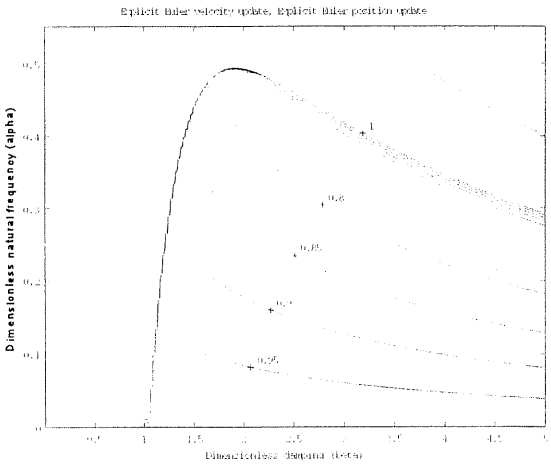

Figure 6. Level curves of the ratio of required damping for the mass simulation to the damping required for a virtual wall. For values less than or equal to one, the system will be passive if (13) is met.

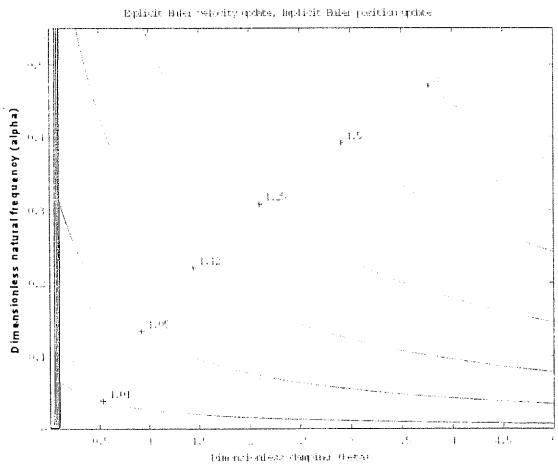

Figure 7. Level curves of the ratio of required damping for the mass simulation to the damping required for a virtual wall. Note that for this integrator, more damping is always required for mass simulations than for wall simulations.

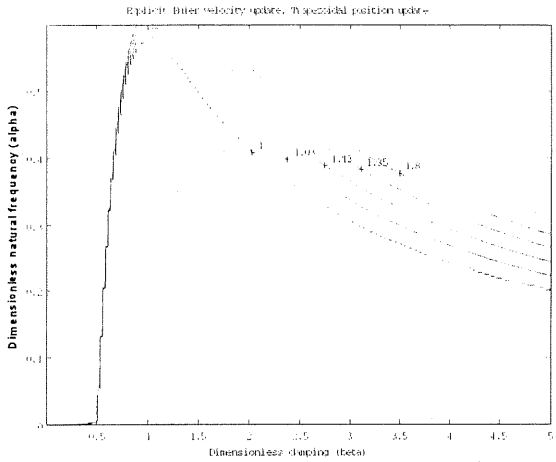

Figure 8. Level curves of the ratio of required damping for the mass simulation to the damping required for a virtual wall. For this integrator, there is a wide region (under the unity level curve) where the required damping exactly matches that of the virtual wall. As long as α and β fall within this region, their values do not affect passivity.

To get a sense for how these restrictions in α-β space affect the dimensioned parameters, one can fit an analytic function to the unity level curve. For Method 3, a reasonable approximation is given by (16), and is shown graphically in Figure 9:

$$\alpha < \frac{\beta}{\beta^2 + 0.732\beta + 0.25}, \quad \beta > \frac{1}{2} \tag{16}$$

Converting (16) back to the dimensioned parameters results in the following three conditions that must be met in order to guarantee passivity of the haptic display:

$$\begin{aligned} b &> \frac{KT}{2} + B \\ B &> \frac{1}{2}KT \\ m &> BT + 0.732KT^2 + \frac{K^2T^3}{4B} \end{aligned} \tag{17}$$

The first condition is simply the normal virtual wall result, the second places a limitation on the virtual damping, and the final indicates a minimum mass that can be simulated safely. The importance of these results is not the exact value of the minimum mass or the quality of the analytic approximation, but rather that the minimum mass exists in the first place. As long as the mass is kept above this value, passivity is guaranteed. This result corroborates our experiences when implementing multibody simulations with a virtual coupling. If the mass (or moment of inertia) drops too low, the system

becomes unstable. If the mass is kept above this minimum, the simulations are exceptionally reliable.

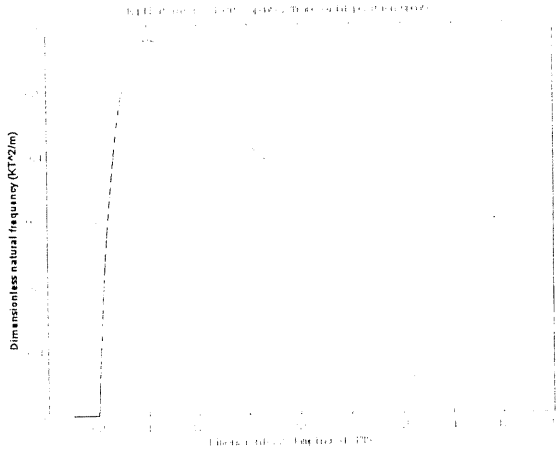

Figure 9. Passivity result for trapezoidal position updates. Values of α below that shown result in a passivity condition that matches that of the virtual wall. The solid line is the actual passivity boundary, while the dashed line shows the approximation given in (16).

4. CONCLUSIONS

The results of the previous section indicate that it is possible to obtain robust performance in multibody simulations, even while using explicit numerical integrators. Constraints are placed on the virtual coupling parameters, along with a restriction on the mass of the virtual tool. When used in conjunction with energy conserving collision response algorithms, the resultant system will remain passive (Brown and Colgate, 1997). This approach allows complex simulations to be built, while maintaining a strong passivity guarantee.

Our findings further suggest that, among the three integration schemes considered, explicit Euler integration for velocity updates coupled with trapezoidal integration for position should allow the widest range of virtual masses to be simulated. Anecdotal evidence agrees with this conclusion, and formal experiments are underway to verify the claim.

Finally, these results suggest a tuning procedure that could be used to ensure reliable behavior for tool-based simulations using a virtual coupling:

- Identify the appropriate virtual stiffness and damping through simulation of virtual walls.
- Identify the minimum mass and moment of inertia associated with the numerical integrator of choice.
- If lower masses are required, then a tradeoff can be made by dropping the virtual coupling stiffness and damping.

This procedure has proven extremely reliable in a planar general-purpose multibody simulator, as written about in (Chang and Colgate, 1997).

5. APPENDIX - PASSIVITY CONDITIONS

Recall from Section 3.3.1 the passivity condition for the virtual wall:

$$b > \frac{KT}{2}(1+2\beta) \tag{A1}$$

where dimensionless parameters α and β are given by:

$$\alpha = \frac{KT^2}{m_e} \qquad \beta = \frac{B}{KT} \tag{A2}$$

Using the transfer functions from Table 1, along with the general passivity result of (8), we obtain passivity conditions for each of the point mass simulations. For Method 1, which uses explicit Euler integration for both velocity and position updates, we find the minimum amount of physical damping necessary to ensure passivity:

$$b > \frac{KT}{2}\cdot\frac{1}{1-\cos\omega T}\cdot \mathrm{Re}\left\{\frac{(1+\beta-\beta z^{-1})(1-z^{-1})^3}{(1-z^{-1})^2+\alpha(1+\beta-\beta z^{-1})z^{-2}}\right\}_{z=e^{j\omega T}} \tag{A3}$$

The resulting condition can be compared to (A1) by examining the coefficient of $\frac{KT}{2}$ for each case. The minimum necessary damping will be less than or equal to that associated with the virtual wall if:

$$1+2\beta \geq \frac{1}{1-\cos\omega T}\cdot \mathrm{Re}\left\{\frac{(1+\beta-\beta z^{-1})(1-z^{-1})^3}{(1-z^{-1})^2+\alpha(1+\beta-\beta z^{-1})z^{-2}}\right\}_{z=e^{j\omega T}} \tag{A4}$$

Method 2 uses an explicit Euler integrator to update velocity and an implicit Euler integrator to update position. Using the same technique as above, the passivity condition of the mass simulation will match that of the virtual wall if:

$$1+2\beta \geq \frac{1}{1-\cos\omega T}\cdot \mathrm{Re}\left\{\frac{(1+\beta-\beta z^{-1})(1-z^{-1})^3}{(1-z^{-1})^2+\alpha(1+\beta-\beta z^{-1})z^{-1}}\right\}_{z=e^{j\omega T}} \tag{A5}$$

As seen in Figure 7, this condition can be met only in the limit as β approaches infinity or if α=0. While simulations using this method can be passive, they will always require more damping than a virtual wall alone.

Method 3 uses an explicit Euler integrator to update velocity and a trapezoidal integrator to update position. Applying the same technique again results in an equation that must be met for the passivity condition of the mass to match that of the virtual wall:

$$1+2\beta \geq \frac{1}{1-\cos\omega T}\,\mathrm{Re}\left\{\frac{\left(1+\beta-\beta z^{-1}\right)\left(1-z^{-1}\right)^{3}}{\left(1-z^{-1}\right)^{2}+\alpha\left(1+\beta-\beta z^{-1}\right)\left(1+z^{-1}\right)z^{-1}}\right\}_{z=e^{j\omega T}} \tag{A6}$$

6. BIBLIOGRAPHY

Adams, R., Moreyra, M. R. and Hannaford, B., 1998, "Stability & performance of haptic displays: Theory and experiments," *International Mechanical Engineering Congress and Exhibition*, ASME, Anaheim, CA.

Brown, J. M. and Colgate, J. E., 1997, "Passive Implementation of Multibody Simulations for Haptic Display," *International Mechanical Engineering Congress and Exhibition*, ASME, Dallas, TX, Vol. DSC-61, pp. 85-92.

Chang, B. and Colgate, J. E., 1997, "Real-time Impulse-based Simulation of Rigid Body Systems for Haptic Display," *International Mechanical Engineering Congress and Exhibition*, ASME, Dallas, TX, pp. 145-152.

Colgate, J. E., Grafing, P. E., Stanley, M. C. and Schenkel, G., 1993, "Implementation of Stiff Virtual Walls in Force-Reflecting Interfaces," *IEEE Virtual Reality Annual International Symposium*, Seattle, WA, pp. 202-207.

Colgate, J. E. and Schenkel, G. G., 1997, "Passivity of a Class of Sampled-Data Systems: Application to Haptic Interfaces," *Journal of Robotic Systems*, Vol. 14, No. 1, pp. 37-47.

Colgate, J. E., Stanley, M. C. and Brown, J. M., 1995, "Issues in the Haptic Display of Tool Use," *IEEE/RSJ International Conference on Intelligent Robots and Systems*, Pittsburgh, Vol. 3, pp. 140-145.

Desoer, C. A. and Vidyasagar, M., 1975, *Feedback Systems: Input-Output Properties*, Academic Press, New York.

Gillespie, R. B., 1996, "Haptic Display of Systems with Changing Kinematic Constraints: The Virtual Piano Action," Ph. D., Stanford University.

Gillespie, R. B., 1997, "A Survey of Multibody Dynamics for Virtual Environments," *International Mechanical Engineering Conference and Exhibition*, ASME, Dallas, TX, Vol. DSC-Vol. 61, pp. 45-54.

Howe, R. D. and Cutkosky, M. R., 1993, "Dynamic tactile sensing: perception of fine surface features with stress rate sensing," *IEEE Transactions on Robotics and Automation*, Vol. 9, No. 2, pp. 140-151.

Klatzky, R., Lederman, S. and Reed, C., 1989, "Haptic Integration of Object Properties: Texture, Hardness, and Planar Contour," *J. of Exp. Psychology: Human Perception and Performance*, Vol. 15, No. 1, pp. 45-57.

Minsky, M. D. R., 1995, "Computational Haptics: The Sandpaper System for Synthesizing Texture for a Force-Feedback Display," Ph.D. Thesis, Media Lab, MIT.

Salcudean, S. E. and Vlaar, T. D., 1994, "On the Emulation of Stiff Walls and Static Friction with a Magnetically Levitated Input/Output Device," *International Mechanical Engineering Exposition and Congress*, C. J. Radcliffe, ed., ASME, Chicago, IL, Vol. DSC 55-1, pp. 303-310.

Zilles, C. and Salisbury, K., 1995, "A Constraint-Based God Object Method for Haptic Display," *International Conference on Intelligent Robots and Systems*, IEEE/RSJ, Pittsburgh.